文章编号：1001－9014(2017)06－0660－05

DOI:10.11972/j.issn.1001－9014.2017.06.005

Optimized coupling loss between single mode fiber and hollow-core photonic crystal fiber for Raman gas detection

ZHANG Xiu-Mei, JIANG Shu-Bo*, WANG Xu

(College of Electrical Engineering and Control Science, Nanjing Tech University, Nanjing 211816, China)

Abstract: In this investigation, the coupling losses caused by Fresnel reflection, core misalignment between single mode fiber (SMF) and HC-PCF are analyzed. A novel solution proposed from this research will reduce the coupling losses by using a T-type tube as a connector. Meanwhile, the theoretically calculated optimized gaps are at 15 μm in SMF-HCPCF direction and 25 μm in HCPCF-SMF direction. Thus, an experiment has been carried out, and the results of the practical gap in the above mentioned two directions have also been obtained. Furthermore, compared with detection by traditional methods, the proposed new detection method with PCF can remarkably enhance the Raman spectroscopy signal. Finally, the prospect of using the combination of HC-PCF and Raman spectroscopy in gas-cell detection has been demonstrated by using oxygen and nitrogen.

Key words: hollow-core photonic crystal fiber, single mode fiber, coupling loss, Fresnel reflection, gas detection

PACS: 87.64.-t, 87.64. Je

空芯光子晶体光纤与单模光纤耦合优化及在拉曼气体检测中的应用

张秀梅, 蒋书波*, 王 旭

(南京工业大学,电气工程与控制科学学院,江苏 南京 211816)

摘要:分析了由菲涅尔反射、中心点偏移引起的耦合损耗.提出了一种新的方法——用T型金属管作为光子晶体光纤和单模光纤的连接器.计算了从单模光纤到光子晶体光纤方向以及从光子晶体光纤到单模光纤方向的最佳耦合距离,分别为15 μm和25 μm,实验证明了结论的可靠性.与传统的检测方法相比,采用光子晶体光纤的检测方法使得拉曼信号得到明显增强. 以氮气为背景气,采用氧气肯定了光子晶体光纤同拉曼检测技术相结合后在气体检测方向的应用前景.

关 键 词:空芯光子晶体光纤;单模光纤;耦合损耗;菲涅尔反射;气体检测

中图分类号:TN253 **文献标识码**:A

Introduction

Photonic Crystal Fiber (PCF)[1] is playing a promising and powerful role in several research and industrial areas due to its distinctive properties, which include photonic band-gap effect, endlessly with single-mode characteristics, and dispersion characteristics. The diversity of these useful properties is not available in conventional fibers, hence PCF is establishing in particular in a good number of applications in ever-widening areas. Nowadays, detection technologies combined with HC-PCF provide new detection methods useful for the industry, medical treatment, and environmental monitoring. The application of HC-PCF in Raman spectroscopy is a novel method for gas detection since it can enhance the sensibility and accuracy in Raman detection, which could result in its various prospective and cost effective applications in photonics in the near future. However, it is difficult in butt coupling between SMF and HC-PCF[2-3]. The coupling loss will occur between fibers which in turn will affect the validity of Raman detection.

Researchers are carrying out extensive investigations focusing on reducing splice loss. Xi Xiaoming *et al.* carried out a feasible solution to decrease the joint loss, which gradually reduced the air-hole collapse of PCFs, i.e. less than 0.3 dB loss[4]. Worldwide, a typical experiment was carried out where fibers were cleaved with

Received date: 2017-05-02, **revised date**: 2017-09-15 **收稿日期**:2017-05-02, **修回日期**:2017-09-15

Foundation items: Supported by National Nature Science Foundation of China (61308066)

Biography: ZHANG Xiu-Mei (1991-), female, Nanjing, master. Research area involves Raman spectroscopy, photonic crystal fiber and laser. E-mail: bhldhd2016@163.com

* **Corresponding author**: E-mail: jiangshubo@njtech.edu.cn

an 8° angle from normal and the HC-PCF was spliced hermetically at both ends to SMF[5].

In the present study, a gas detection system has been designed with HC-PCF sample pool. Then, Raman detection is validated using this system. For this purpose, a T-type metal tube was utilized in fiber coupling between SMF and HC-PCF. Though the losses are inevitable, both the theoretical analysis and experimental results have shown that the highest coupling efficiency exists in the optimal distance of two fibers. Moreover, while comparing with traditional detection, the present experimental results show that Raman spectroscopy signal is enhanced remarkably with PCF.

1 Principle and experiments

1.1 Splice joint technique and optimized gap calculation

Two fibers were SMF (780 HP)[6] and HC-PCF (HC-800B)[7] from NKT Photonics. The parameters of two fibers have been shown in Table 1.

Table 1 Properties of HC-PCF (HC-800 B) and SMF (780 HP)

表 1 HC-PCF (HC-800 B) 和 SMF (780 HP)的特性

Properties	HC-800B	780HP
Operating wavelength	770 ~ 870 nm	780 ~ 970 nm
Core diameter	(7.5 ± 1) μm	4.4 μm
Mode field diameter(MFD)	(5.5 ± 1) μm	(5.0 ± 0.5) μm
Numerical aperture(NA)	0.2	0.13
Attenuation	<250 dB/km	<3.5 dB/km

It is a tough technique to splice both ends of HC-PCF to SMFs with dissimilar parameters such as Mode-field diameter (MFD), numerical aperture (NA), and core diameter. Some of the splicing techniques such as filament fusion with continuous laser illumination and fusion splicing have been reported previously[8-10]. However, their disadvantages in splicing either led to high coupling losses or made air-hole collapsed. An idea using a stainless-steel tube to connect HC-PCF with SMF was also mentioned[11]. However, it is merely confined between SMF and solid core PCF. In the current work, a T-type metal tube is utilized not only as a connector to join SMF and HC-PCF but also as a gas cell. The proposed structure is shown in Fig. 1.

The manufacturing process of T-type tube has two procedures. Depending on their different characteristics, corresponding installation processes were designed accordingly. A novel method was utilized where a hole was drilled firstly with the required size. However, in this procedure the confinement will increase when it comes to distort the tube structure. Then, the hole is flanged by using a spinning blade which can accurately relocate the hole. Alignment of the center is controlled with the help of boring machine. This procedure possesses strong applicability and generality.

From this construction, the splice of the fibers was fixed in alignment and the gaps between fibers were considered in the optimization for distance. The two fibers

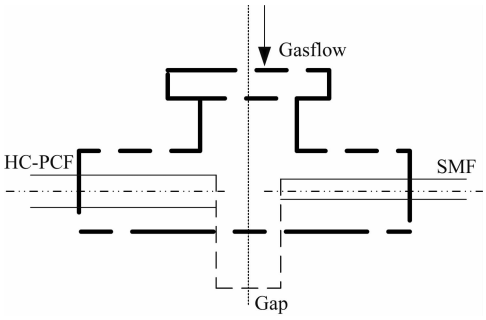

Fig. 1 The proposed T-type structure

图 1 T-型管的结构示意图

are assumed to be parallel to each other. One of the fibers (HC-PCF) guiding at 785 nm was cleaved and then was put into the tube. At the end facet, the other fiber (SMF) was inserted with an optimized gap. After filled with mixture gas (N_2 and O_2), the fibers are stringently sealed. The same technique was followed with SMF-HCPCF. In the later experiment, two sealed tubes were considered as gas cells to control gas filling progress. Moreover, this splicing technology with T-type tube was compact, portable, and especially offered no damage to air hole.

With a view to maximum optical power coupling, these fibers were ultimately spliced with an optimized gap under the condition of dissimilar physical and optical parameters. With this gap, 98% light could transmit through the fiber core. During splice coupling, beams emanating from transmitting fiber get diffracted owing to Fresnel diffraction before launching into the receiving fiber. Light transmitting from HC-PCF or SMF has the similar Gaussian profile. The Gaussian beam diameter is described as MFD and its Petermann-II formula is given as follows:

$$\mathrm{MFD} = 2\omega_0 \quad , \quad (1)$$

where, ω_0 is the spot size of the emanating beam. Light beam propagates along the z-axis. Owing to Fresnel diffraction, the diffraction beam spot size $\omega(z)$ is defined[12]. Where, λ is the source wavelength, z is the optimized gap between HC-PCF and SMF, which is indicated in Fig. 2.

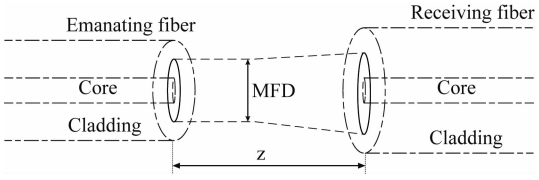

Fig. 2 Gap mode between two fibers

图 2 两个光纤之间的间隙模型

The optimum air gaps "z" between HC-PCF and SMF were computed under the condition of dissimilar MFD, NA and fiber core diameter. Two directions' gaps (from HC-PCF to SMF and from SMF to HC-PCF) were calculated respectively and the calculated results of the gaps are given in Table 2:

Table 2 The optimized distance of fiber coupling
表 2 光纤耦合的优化距离

Direction	λ	ω_0	$\omega(z)$	optimized gap
SMF-HCPCF	785 nm	5.2 μm	5.25 μm	15 μm
HCPCF-SMF	785 nm	3.75 μm	4.1 μm	25 μm

In Table 2, the z value calculated for SMF-HCPCF was 15 μm and for HCPCF-SMF was 25 μm, which ensured that the maximum transmission optical coupling efficiency was up to 98% of the source light.

1.2 Analysis of coupling loss at splice joint

1.2.1 The core misalignment

During the process of coupling splice, the two fibers were aligned hypothetically at a distance "z" from each other. In an implementation, model mismatching occurred where central point deviated "Δr" at one of the end facets. Eventually, serious coupling loss would be caused due to the mismatching mode and for not collimating two fibers when emitting light transmitted from fiber 1 to fiber 2. The cross-section of the fiber's central deviation is depicted in Fig. 3.

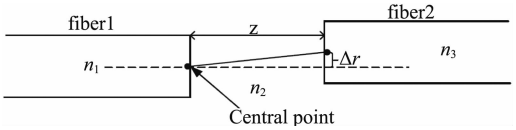

Fig. 3 The deviation of the fiber center
图 3 光纤之间的中心偏移模型

Considering that "z" is the distance between the two fibers, and central deviation is presented inevitably for the beam light that transmits along x-axis and y-axis from one fiber to the other fiber. The related transmission efficiency is achieved when the coupling loss exists. To summarize, fixing the center aperture of fiber reduces the coupling joint loss implicitly and the relationship with θ and z is related to transmission efficiency.

1.2.2 Fresnel loss

Another non-ignorable coupling joint loss exists in fibers' end facets, which is considered as Fresnel loss[13]. In such a coupling joint, emanating beam light propagates from fiber 1 to fiber 2 and its reflection loss at fiber 2 plays a vital role. In Fig. 4, co-directional light beam transmits from medium n_1 through medium n_2 and then hits fiber 2, and finally arrives in medium n_3 partially. The beam hitting at the end facet of fiber 2 experiences reflection loss, which is called Fresnel loss.

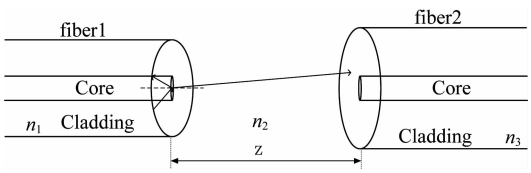

Fig. 4 Scheme to show the Fresnel loss
图 4 菲涅尔损耗结构示意图

The corresponding Fresnel loss is computed using an expression[13]. Researchers previously found solutions to nullify the Fresnel loss at coupling splice. One of these results is to coat the fibers which can only used in SMF-HCPCF. The Fresnel loss should be taken into consideration strictly. The majority of the Fresnel loss at the fiber facet can be avoided as in this research while the HC-PCF used serves as a sample pool, the Fresnel loss should be taken into consideration strictly.

1.3 Experimental configuration

1.3.1 Optimized gap detecting setup

The experimental gaps in the two directions were manifested by using a photodetector. The experimental setup employed is shown in Fig. 5. A light source of 785 nm was launched from SMF to one end of HC-PCF, then transmitted from the other end of HC-PCF to SMF. The optical power was monitored by a detector and the light output was detected at the same time. Therefore, the optimized gap1 between SMF and HC-PCF and gap 2 between HC-PCF and SMF were observed simultaneously when the power output reached to a maximum value. In this configuration, it is vital to ensure the alignment of the centers of SMF and HC-PCF, which produces a maximum power output. The same result could be achieved with HC-PCF and SMF.

Fig. 5 The setup for optimized gap detection
图 5 最优间隙检测装置框图

1.3.2 Gas detecting configuration

After optimizing the optical coupling components, an experimental model for detecting Raman gas was setup as shown in Fig. 6.

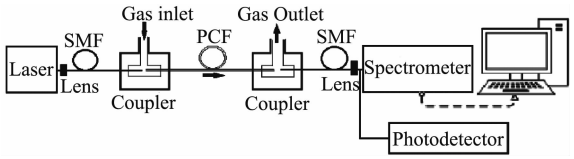

Fig. 6 The fundamental scheme of the detecting system
图 6 光子晶体光纤拉曼气体检测系统基本结构

This system consists of optical devices and gas cells. In optical devices, the laser is a continuous source of power 100 mW at a wavelength of 785 nm. The light beam was aligned using 18 mm focal length aspheric lens (C280TME-A, Thorlabs). SMF (780HP, NKT Photonics) was utilized (operating wavelength ranges within 780 ~ 970 nm where the attenuation is <3.5 dB/km) to splice coupling with a HC-PCF (HC-800B, NKT Photonics where the designed wavelength is centered at 800 nm and its attenuation is less than 250 dB/km). The two fibers were coiled for a compact format and they joint splice with gas cells to lead the gas in and out. The discrepancy was caused by the difficulty in optimizing the coupling splice gap between HC-PCF and SMFs. These optimized gaps, 15 μm from SMF to HC-PCF direction and 25 μm from HC-PCF to SMF direction, were calculated in the research mentioned above. At the end of the second SMF, the transmitted beams were focused in aspheric lens with a 15 mm focal length (C260TME-A,

Thorlabs) onto a spectrometer (HR4000, Ocean Optics) detecting the Raman signal. Eventually, the collected Raman intensity was analyzed by the computer online. Meanwhile, the experimental gaps in two directions (one is from SMF to HC-PCF and the other is from HC-PCF to SMF) were manifested by a photodetector. Furthermore, the two gas cells, consisting of HC-PCF and SMF by a T-type tube can achieve optimized detection efficiency and a maximum detection power.

At last, this gas detection system was characterized quantitatively by choosing nitrogen as reference; the detectable concentrations for oxygen were 3%, 1.5%, 0.5% and 0.1%.

2 Results and discussion

2.1 Optimized gap at the splice interface

Figures 7-8 show the gap data acquired from the experimental device using HC-800B and 780HP, respectively. There is no doubt that a great deal of loss generates from Fresnel reflection at the end face of fibers. Further, the Raman signal is reduced, which necessitates an action to acquire an optimized gap. With the receiving fiber moving away, the return loss is reduced and interference is decreased. Thus, Raman signal can be improved efficiently.

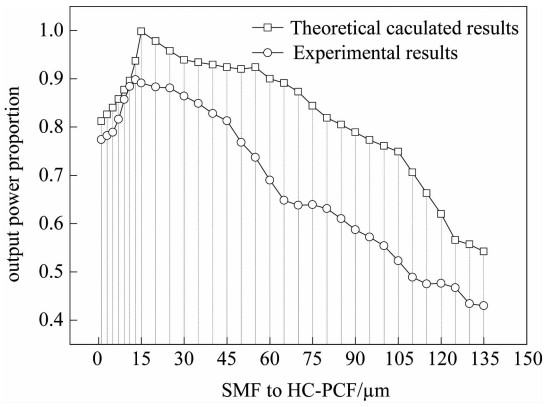

Fig. 7　Comparative theoretical model and experimental results for SMF to HC-PCF
图 7　SMF-HCPCF 方向理论模型与实验结果对比

Figures 7-8 indicate that the output power at zero distance from SMF to HC-PCF direction is more than that obtained from HC-PCF to SMF direction. In Fig. 7, an initial output power shows a low value and it increases gradually as the distance increases. Then, it starts to decline after the maximum output power is achieved. The figure shows that the calculated theoretical value is 15 μm whereas the experimentally obtained value is 14 μm, which indicates that the experimental result is close to the theoretical value. At the maximum gap, both Raman signal and output power achieve optimal results in this configuration. The experimental value in Fig. 8 is approximately 25 μm, which is similar to the calculated theoretical result. This technique is rather compact and easily achievable, beyond what other techniques offer; where the optimized gaps are approximately to 14 μm in SMF to HC-PCF configuration and to 25 μm in HC-PCF to SMF configuration.

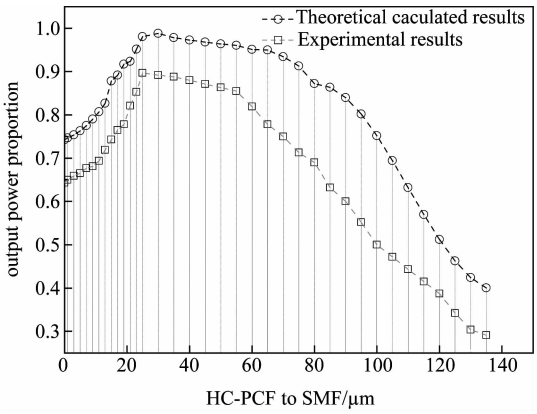

Fig. 8　Comparative theoretical model and experimental result for HC-PCF to SMF
图 8　HCPCF-SMF 方向理论模型与实验结果对比

2.2 Comparison of traditional and PCF detection

Figures 9-10 present the Raman spectroscopy measured by conventional detection technique and by 30 cm long HC-PCF detection technique, respectively. We chose nitrogen (70% at 1 bar) as reference gas and used oxygen (30% at 1 bar) with HC-PCF to achieve a Raman intensity of 20062.733 with a detection time 100 s, whereas the conventional detection technique without HC-PCF only obtained an intensity of 163.305. From the above experimental results, it was observed that Raman signal with HC-PCF could be enhanced 100 times more than the signal obtained by the conventional detection technique.

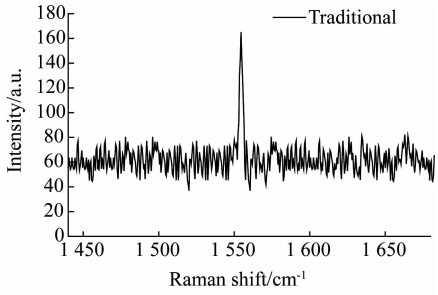

Fig. 9　Raman detection without HC-PCF
图 9　传统的拉曼检测

2.3 Detection at various low concentrations of oxygen

In order to demonstrate the feasibility of this gas-cell detection system, a kinetic series of Raman signal was obtained during filling the 30 cm long HC-PCF with oxygen. Raman shift in oxygen appeared at 1556 cm^{-1}. The gas at 1 bar was used in this experiment. The detectable concentration for oxygen was 3% and for nitrogen was 97% with 30s integrated times. Similarly, other experiments were implemented (O_2 was 1.5%, 0.5%, 0.1% while N_2 was 98.5%, 99.5%, 99.9%). The Raman spectrum of O_2 is shown in Fig. 11. It concludes that for the 785 nm pump, Raman signal intensity increases as the concentration of the gas increases.

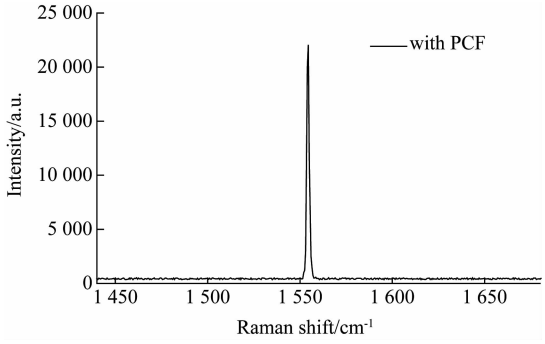

Fig. 10 Raman detection with HC-PCF
图 10 基于光子晶体光纤的拉曼检测

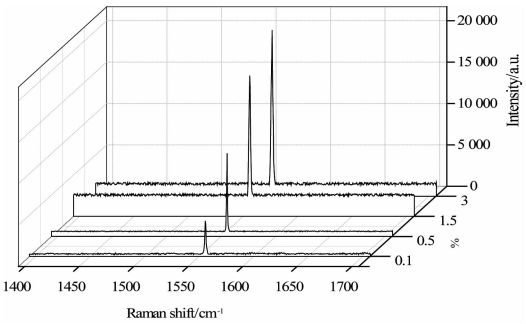

Fig. 11 The detection results at various low concentrations of O_2
图 11 不同气体浓度下的检测结果

We quantitatively analyzed the length dependence of the Raman signal intensity using the HC-PCF. As shown in Fig. 12, the Raman signal intensity increases almost linearly with an increase in the fiber length in the range of 5 ~ 30 cm. The length beyond 30 cm limits the enhancement of Raman signal intensity. Therefore, from these results, it is clear that Raman signal at different concentrations can be achieved by using the detection system proposed in this study, particularly at low concentration.

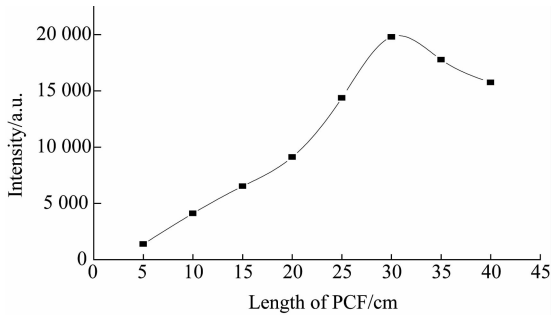

Fig. 12 Relationship between length of PCF and intensity of Raman signal
图 12 拉曼信号随光子晶体光纤长度变化趋势图

3 Conclusion

We hereby successfully report a compact and inexpensive gas detection system based on HC-PCF filling with a mixture of oxygen and nitrogen gases. The difficulty in coupling splice joint between SMF and HC-PCF was mitigated with a T-type tube as a connector. The optimized gaps in two directions were obtained and the results were 15 μm in SMF-HCPCF direction and 25 μm in HCPCF-SMF direction theoretically. Meanwhile, the experiments were carried out to comply with the theoretical values. Compared with the conventional detection method, the signal intensity of Raman Spectroscopy with PCF was enhanced evidently. The O_2 at 3%, 1.5%, 0.5%, 0.1% concentrations were filled in HC-PCF to explore the possibilities of using this detection system. HC-PCF offers an excellent optical characteristic as a gas cell to enhance the Raman signal. However, further investigation into the possibilities of the proposed system could be considered to bring more development.

References

[1] Russell P. Photonic crystal fibers[J]. *Science*, 2007, **299**(12):4729 -4749.
[2] Wang E, Jiang H, Zhang J. Low-loss coupling between photonic crystal fibers and single-mode fibers[J]. *Optik - International Journal for Light and Electron Optics*, 2016, **127**(11):4755 -4757.
[3] Nicholson J W, Meng L, Desantolo A. Low-loss, low return-loss coupling between SMF and single-mode, hollow-core fibers using connectors[C]. Lasers and Electro-Optics. IEEE, 2014:1 -2.
[4] XI Xiao-Ming , CHEN Zi-Lun, LIU Shi-Yao, *et al*. Coupling and fusion splicing of photonic crystal fiber with conventional fibers[J]. *Laser Technology*(奚小明,陈子伦,刘诗尧,等. 光子晶体光纤与普通光纤的耦合熔接. **激光技术**). 2011, **35**(2):202 -207.
[5] Couny F, Benabid F, Light P S. Reduction of Fresnel back-reflection at splice interface between hollow core PCF and single-mode fiber[J]. *IEEE Photonics Technology Letters*, 2007, **19**(13):1020 -1022.
[6] HC-800B HC-PBF datasheet acquired in 2017. 4. 14. https://www.thorlabschina. cn/thorproduct. cfm? partnumber = HC-800B.
[7] 780HP SMF datasheet acquired in 2017. 4. 14. https://www. thorlabschina. cn/thorproduct. cfm? partnumber = 780HP.
[8] Chow K K, Short M, Lam S, *et al*. A Raman cell based on hollow core photonic crystal fiber for human breath analysis[J]. *Medical Physics*, 2014, **41**(9):092701.
[9] Benabid F, Knight J C, Antonopoulos G. Stimulated Raman scattering in hydrogen-filled hollow-core photonic crystal fiber[J]. *Science*, 2002, **298**(5592):399 -402.
[10] Benabid F, Couny F, Knight J C, *et al*. Compact, stable and efficient all-fiber gas cells using hollow-core photonic crystal fibers[J]. *Nature*, 2005, **434**(7032):488 -91.
[11] Li X, Liang J, Zimin Y, *et al*. U-Band wavelength references based on photonic bandgap fiber technology[J]. *Journal of Lightwave Technology*, 2011, **29**(19):2934 -2939.
[12] Parmar V, Bhatnagar R, Kapur P. Optimized butt coupling between single mode fiber and hollow-core photonic crystal fiber[J]. *Optical Fiber Technology*, 2013, **19**(5):490 -494.
[13] Farsinezhad S, Seraji F E. Analysis of Fresnel loss at splice joint between single-mode fiber and photonic crystal fiber[J]. *International Journal of Optics*, 2012, **2**(1):17 -21.